www.czasopisma.pan.pl PAN www.journals.pan.pl
Opto-Electronics Review 27 (2019) 123–129

Contents lists available at ScienceDirect

Opto-Electronics Review

journal homepage: http://www.journals.elsevier.com/opto-electronics review

Full Length Article

Measurements of the responsivity of FET-based detectors of sub-THz radiation

P. Kopyt [a,*], B. Salski [a], A. Pacewicz [a], P. Zagrajek [b], J. Marczewski [c]

[a] Inst. of Radioelectronics and Multimedia Technology, Warsaw University of Technology, ul. Nowowiejska 15/19, 00-665, Warsaw, Poland
[b] Inst. of Optoelectronics, Military University of Technology, ul. gen. Witolda Urbanowicza 2, 00-908, Warsaw, Poland
[c] Institute of Electron Technology, Al. Lotnikow 32/46, 02-668, Warszawa, Poland

ARTICLE INFO

Article history:
Received 22 December 2018
Accepted 8 April 2019
Available online 7 May 2019

Keywords:
Lenses
Electromagnetic analysis
Submillimeter wave detectors
Responsivity

ABSTRACT

This article describes a novel approach to measure responsivity of a FET-based sub-THz detector using on-wafer probes to directly feed a bare antenna-less detecting device. Thus, the approach eliminates the need to know beforehand the detector's effective aperture, which can be a source of large variation between responsivity measurements of various FET-based detectors often cited in the literature. It seems that the presented method can be useful at making direct comparisons between responsivity of various devices (e.g., MOSFETs, HEMTs etc.). As a demonstration, the sub-THz responsivity of a pHEMT device fabricated using a commercial GaAs process has been measured in a WR-3 frequency band. Additionally, the results have been compared against data obtained using an alternative approach. The verification method consisted in integrating exactly the same device with a broad-band antenna and a carefully selected high-resistivity silicon lens and comparing its performance with that of a commercial calibrated detector based on Schottky diodes.

1. Introduction

The publication of the Dyakonov-Shur (DS) [1] theory predicting the possibility of detecting sub-THz radiation with a Field-Effect-Transistor (FET) motivated the scientific community to investigate effects occurring in the channel of FET devices employed as cheap imaging detectors that could be used in a number of areas. In the case of such structures one observes usually the so-called non-resonant detection, where the phenomenon of rectification of THz-band signals may be explained with classical resistive mixing theory with a number of extensions as described in Ref. 2. FET devices employed as detectors in this frequency range are often compared to existing and wide-spread semiconductor-based detecting structures like superconductor–insulator–superconductor tunnel junction devices (SIS) [3] or the Schottky diodes [4]. However, such comparisons become a very demanding task because there seems to exist a large discrepancy between responsivities of FET-based detectors reported by various research groups active in the area even with respect to devices fabricated with very similar technologies and measured in comparable frequency ranges, which was very as briefly addressed in Ref. 5.

It seems that there is one fundamental reason for this. Typical set-ups employed in such measurements consist of a sub-THz source that illuminates a device-under-test (DUT), that can be a bare antenna-less device or a structure integrated with some radiator. In order to accurately measure responsivity of such structures, a DC biasing must be applied as the Gate-Source voltage (V_{GS}) because the maximum responsivity is usually observed when the V_{GS} voltage is kept close to the turn-on voltage of the transistor [6]. The input sub-THz signal of the known power level (P_{in}) is usually delivered to the Gate of the structure, also. In typical set-ups the photo-detection signal (the response) is recorded as the voltage V_{DS} measured between the Drain and the Source electrodes of the DUT. Otherwise, the output is left open (unbiased) and all the biasing and the output signals are typically applied, or are available for measurements, through bond-wires. An estimation of the responsivity given in (V/W) is obtained by measuring the V_{DS} output voltage and calculating the input power P_{in} on the basis of known power density of the electromagnetic (EM) wave illuminating the structure and the effective aperture A_{eff} of the detector (either antenna-less or integrated with a dedicated antenna). However, as shown in Ref. 7, even bond-wires can effectively act as unintended antennas of barely known characteristics depending on the accuracy/repeatability of a bonding process. As a result the amount of power P_{in} that actually reaches the DUT is rather unknown and can only be roughly approximated.

* Corresponding author.
E-mail address: pkopyt@ire.pw.edu.pl (P. Kopyt).

https://doi.org/10.1016/j.opelre.2019.04.001
1230-3402/

Table 1
Comparison of responsivities of the selected sub-THz radiation detectors based on FET transistors.

Technology	Freq. [GHz]	Device Responsivity	Additional amplifier	Method to estimate the responsivity	Ref.
250 nm NMOS SiGe (IHP)	600	250 V/W	140 V/V	Purely analytically.	[8]
65 nm CMOS Si (STM)	1027	10 V/W	80 V/V	By measurements but A_{eff} of each pixel estimated based on its surf. area and the directivity of the antenna.	[9]
65 nm CMOS Si (STM)	650	13.75 V/W	80 V/V	By measurements but A_{eff} of each pixel estimated based on the simulated directivity of its antenna.	[12]
150 nm CMOS Si (LF)	600	350 V/W	–	By measurements but A_{eff} of each pixel estimated based on its surf. area.	[2]
130 nm CMOS Si (STM)	300	2600 V/W	35 V/V	By measurements but A_{eff} of each pixel estimated based on its surf. area.	[10]
130 nm NMOS SiGe (IHP)	650	450 V/W	–	By measurements but A_{eff} of each pixel estimated based on the surf. area of the lens.	[11]

The situation when a detecting device is integrated with a carefully designed antenna is only marginally better. In those cases the amount of power that reaches the DUT is not measured directly either. Instead, similarly to the previous case, it must be also approximated with various estimates of A_{eff}. Some reported values are listed in Table 1. In some publications, as in Ref. 8, the aperture is estimated analytically. In other representative publications [2,9,10] the authors also neglected any wires and simply used the surface area of the detector (or a lens integrated with it) as A_{eff}. In Ref. 11 A_{eff} was determined by means of EM numerical modeling of the antenna integrated with the transistor. Regardless of which method was employed to estimate the responsivity of a detector, the result is nearly always burdened with a large systematic error depending on the choice of A_{eff}. As a result, very similar devices (NMOS FETs with a characteristic distance of 65, 130 or 150 nm) are reported as sub-THz detectors with responsivities at ca. 600 GHz ranging from 10 to 13 V/W [9] through 350–400 V/W [2,11] up to values as high as 2600 V/W [10]. The detector reported in Ref. 6 has been characterized at 300 GHz, but it has been integrated with an antenna of dimensions adjusted to 600 GHz, and for this reason it has been accounted for in the comparison. These discrepancies in the reported responsivity values for comparable transistors without any particular modifications of their construction raises questions about credibility of characterization methods employed in those cases and similar ones.

A very accurate approach to answer such questions was reported in Ref. 4. It consists in augmenting with additional measurement data some free-space responsivity measurements of a detector built of a DUT integrated with a well defined antenna. By separately measuring the same DUT integrated with different focusing structure (e.g., an open-ended waveguide or a horn antenna) one can gather accurate data on the responsivity of the DUT alone, as well as the A_{eff} of the antenna. The major drawback of the approach is an added difficulty of integrating the DUT with a waveguide, which can be expensive, particularly, when several DUTs need to be characterized and subsequently compared.

For this reason, in this paper we have focused on measuring responsivity of FET-based detectors of sub-THz radiation using two different approaches that are easier to implement in practice than the one presented in Ref. 4. The proposed methods do not employ arbitrary coefficients that are sometimes used in such measurements and the presence of which makes in practically impossible to directly compare responsivities of various devices measured by different research groups. To the best knowledge of the authors no similar reports have been published in the literature. Thus, the goal of this paper is to point this out by suggesting two alternative approaches and, possibly, to open within the community a discussion on the most reliable methods of comparing properties of various FET-based structures employed as (sub-)THz radiation detectors.

The first of the proposed methods – described in Section 2. – has been already briefly presented in ref. 13 and consists in performing a set of sub-THz on-wafer measurements of DUTs and it does not require any arbitrary assumptions. By providing the input sub-THz power to a DUT using on-wafer probes the structure's responsivity in (V/W) can be extracted in a very straightforward manner allowing for rapid characterization and direct comparisons between multiple structures. Using this method we have measured responsivity of HEMT devices fabricated with a commercial process. The results are compared to data obtained with a second approach – presented in Section 3. – which has been shortly described in Ref. 14. The approach uses a reference free-space detector of known responsivity calibrated by its manufacturer with the method reported in Ref. 4. The reference structure is compared to a custom-made detector of sub-THz radiation constructed of the same HEMT device as the one characterized using the first method. However, in this approach the transistor has been monolithically integrated with a log-periodic broad-band planar antenna mounted on a low-loss (high-resistivity, HR) silicon (Si) lens. As a result, an unknown detector coupled to free-space has been obtained. Both the detectors employ HR lenses of similar dimensions. Thus, by directly comparing the raw data on the amplitude of the signal measured at the output of each of the detectors the responsivity of the unknown structure can be found. Similarly to the method based on on-wafer measurements, also the comparative approach does not require using any arbitrary coefficients, as A_{eff}. The results of the both methods are compared in Section 4. together with a discussion.

2. The on-wafer method to measure responsivity

A measurement set-up employed for the proposed on-wafer measurements is shown in Fig. 1(a) . Its major component is a custom-made on-wafer probing station presented in Fig. 1(b) which has been used to position the on-wafer ground-signal-ground (GSG) probes onto a sample. In our measurements we have used probes operating in the WR-3 frequency band (220÷330 GHz) from DMPI, Inc. A sub-THz signal source (the amplifier-multiplier chain AMC-10 unit from VDI, Inc.) was providing ca. 1 mW monochromatic incident wave of frequency selectable in the band of 200÷350 GHz. The signal was feeding the on-wafer probe touching the input of the DUT, i.e. the metallization pads connected to the Gate and the Source of the DUT as shown in Fig. 1(c). The DUT is designed in the so-called π-configuration, where two transistors are connected in parallel. The Source electrodes of the devices are located at the edges of the structures while in the middle one finds the metallization pad of the Gate (at the input) or the Drain (at the output). Such a configuration is often employed in on-wafer characterization of devices as it is naturally compatible with symmetrical construction of the GSG on-wafer probes.

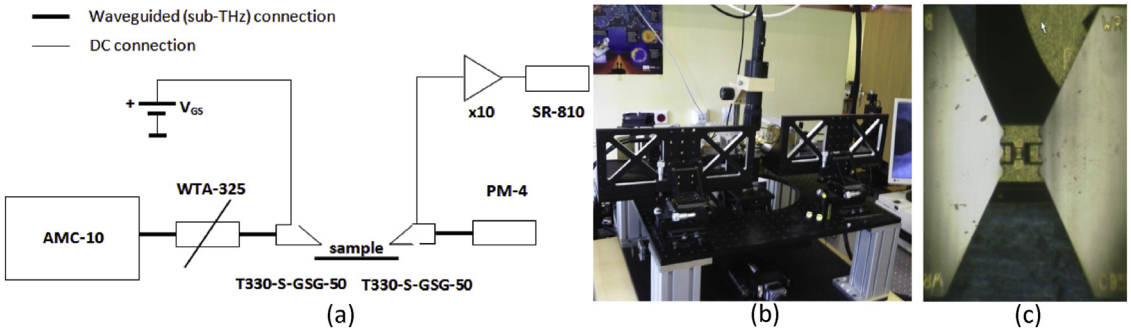

Fig. 1. A schematic view on the measurement set-up for on-wafer responsivity testing (a); a general view on the custom-made on-wafer station with large XYZ micrometer positioners employed to hold the source of the sub-THz signal (b) and a photograph showing two GSG on-wafer probes touching the metallization layer of a HEMT transistor in π-configuration (c).

The bias-T built into the input probe allowed providing the DC-bias – the V_{GS} voltage – to the DUT's Gate and eliminated any need for additional wire-bonded connections. At the output of the DUT (i.e., the Drain) we have used a similar on-wafer GSG probe that has been directly connected to a power meter (Ericsson PM-4 from VDI, Inc.). The power meter has provided a matched termination of the output. Also, it provided information that helped to evaluate transmission losses resulting from a non-perfect contact between the metallization pads of the DUT and the probes. The bias-T of the output probe provided an access to the photo-detection signal available at the output as the V_{DS} voltage.

The photo-detection signal was fed to a lock-in amplifier (SR-810 from Stanford Research Systems, Inc.) synchronized with a low-frequency chopping signal that was modulating the sub-THz source during measurements. In order to avoid driving the detector into saturation, a 10 dB waveguide attenuator (WTA-325 from Radiometer Physics, GmbH) has been added between the sub-THz source and the input probe. This not only limited the power fed into the DUT but also eliminated reflections from the non-matched DUT's input. The probes were positioned on samples using a digital microscope (Keyence VH-Z35 lens with the 7000-series processing unit) with its lens mounted on a custom stand of adjustable observation height. Using the set-up, a responsivity R of a DUT can be obtained with the following equation:

$$R = \frac{\Delta U}{P_{in}}, \tag{1}$$

where ΔU is the photo-detection signal available at the output probe as the U_{DS} voltage while taking into account the presence of a low-noise pre-amplifier (x10 gain), and P_{in} is the power delivered to the active part of the transistor defined as:

$$P_{in}(f) = P_{source}(f)\left|S_{21}^{Att}(f)\right|^2\left(1 - \left|S_{11}^{FET}(f)\right|^2\right), \tag{2}$$

where P_{source} is the power delivered by the sub-THz source with all necessary corrections, ${S_{21}}^{Att}$ is the attenuation of the WTA-325 attenuator (fixed at 10 dB during our measurements), while ${S_{11}}^{FET}$ is the reflection coefficient of the DUT, measured separately with a vector network analyzer (VNA) and a set of frequency extenders and on-wafer probes calibrated so that the reference plane of the measurement is shifted to the probe tips only. Measuring the reflection coefficient is necessary because a bare transistor is poorly matched to characteristic impedance of the probes and a considerable amount of power is reflected from the device. Without taking the reflections into account, the responsivity R would be lower than the real value.

Although the power level at the signal source is well known and controlled at each frequency point, the insertion loss of the input probe, and especially, the quality of the contact between the probing tips and the probing pads of the DUT can vary, which affects the amount of available power. The readings from the PM-4 power meter obtained when measuring some straight sections of transmission lines (i.e., THRU) that had been fabricated on the same wafer has made it possible to verify the quality of the contact. The attenuation due to the finite quality of contacts, as well as the insertion losses of the input probe itself raises the value of ${S_{21}}^{Att}$ in Eq. (2) above the nominal 10 dB. Accounting for this effect by adding necessary corrections to the ${S_{21}}^{Att}$ coefficient reduces the systematic error of the measurements.

3. Responsivity measurement by the comparative method

In order to verify the method described in the previous section, another approach has also been tested. A dual-gate HEMT of channel width of 30 μm, which is exactly the same as the device selected for on-wafer tests described in the previous Section, has been integrated with a log-periodic antenna [15] located on a topmost metallization layer. The layout of the structure is presented in Fig. 2(a), where the antenna metallization plane is shown in blue. The complete structure has been designed and fabricated within the PH-10 GaAs pHEMT process offered commercially by United Monolithic Semiconductors S.A.S (UMS). The bare chip is shown in Fig. 2(b), while Fig. 2(c) presents a complete detector constructed with the chip and a HR silicon lens of appropriate dimensions as discussed in the next Section. The antenna directly feeds the Source and the Gate contacts of the HEMT as defined in Fig. 2(a). The DC-bias voltage, as well as the photo-detection signal has been applied, or measured, through the arms of the antenna. The V_{DS} voltage is accessible at contact pads located near the outer edge of the lower arm of the antenna.

The responsivity measurement requires that the photo-detection voltage ΔU_{HEMT} of the HEMT-based detector illuminated with a sub-THz signal generated by a sub-THz signal source is measured. Then, the same set-up has been used again to record the photo-detection signal ΔU_{REF} of a calibrated commercial quasi-optical Shottky-based detector of known responsivity R_{REF}. In our case we have used the QOD 1–14 from VDI, Inc. as the reference structure. In both cases the same distance (ca. 30 cm) between the detector and the signal source has been maintained, as well as the output power of the signal. In the measurement set-up a lock-in amplifier (the SR-810 unit) synchronized with a low-frequency chopping signal modulating the sub-THz source during measurements has been employed in order to improve the signal-to-noise ratio. As the signal source the AMC-10 system has been used, again. In this method the responsivity R of the unknown structure is obtained with the straightforward equation:

$$R = R_{REF}\,\Delta U_{HEMT}/\Delta U_{REF}. \tag{3}$$

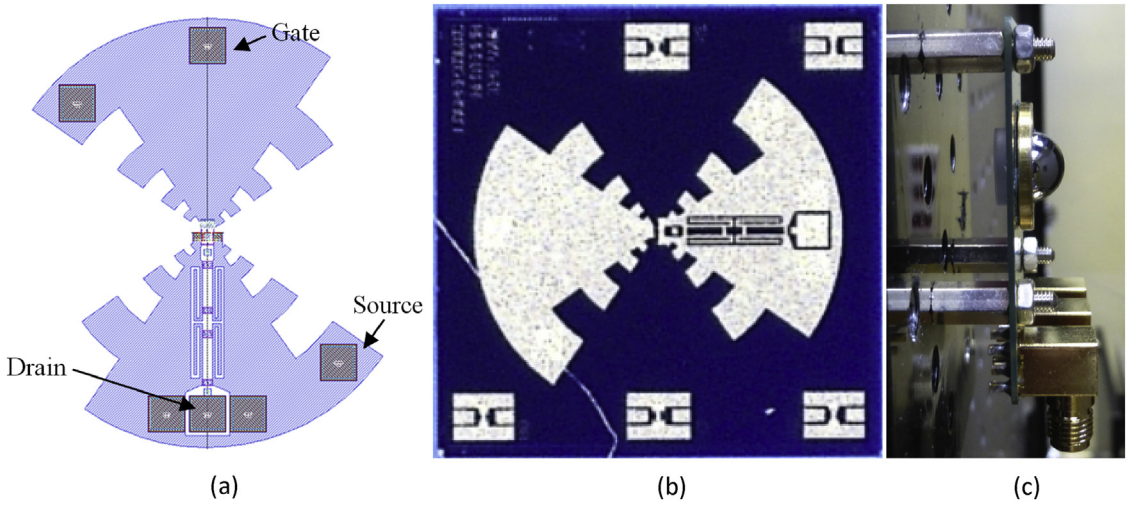

Fig. 2. A custom-made sub-THz detector built of a GaAs HEMT integrated with a log-periodic antenna: the layout (a); a photograph of fabricated device (b); and a detector built of the device and a HR lens (c).

4. The design of a HR lens

The lens attached to a radiation detector built of our HEMT device is responsible to increase the effective aperture A_{eff} of the structure so that it is large enough to receive, ideally, all power emitted from the source. In the comparative method described in the previous Section the illuminating signal is radiated through a horn antenna of 3-decibel beamwidth of 10° [16] at the frequency of 270 GHz (the center of the WR-3 band). At a distance of 30 cm the diameter of the Gaussian beam is ca 5.2 cm. Employing silicon lenses of comparable size would make the experiment prohibitively expensive. However, any lenses of a diameter smaller than this dimension receives only a fraction of the emitted power, and even a slight increase of the aperture would significantly improve the photo-response. For this reason the lenses integrated in both detectors employed in the experiment had the same diameter of 10 mm. Otherwise we would have to account for the difference between their effective apertures while comparing their photo-detection signals.

It is well known [17] that the most optimal lens that can be integrated with a planar antenna in order to improve its effective aperture is the elliptical one. The exact shape of such lenses depends on the electric permittivity material they are made of. However, the higher the permittivity of the material the more spherical become the lens. For this reason it is feasible to synthesize semi-optimal lenses simply by employing a hyper-spherical lens or by integrating a hemi-spherical lens with a cylindrical post of proper height leading to the so-called extended hemispherical lens. There can be proposed a number of criteria to design such semi-optimal lenses. The authors of Ref. 18 used a procedure based on a least-squares fit of the spherical lens to the elliptical one. We have used the same procedure to design lenses to be employed in our detectors.

The results of such a procedure applied to exemplary lenses made of HR-Si are shown in Fig. 2(a) where a hemispherical lens has been extended with a post in order to bring the flat bottom of the resulting lens to the plane where the lower focus of the reference elliptical lens is located. A three-dimensional (3D) full-wave numerical model of the scenario has been built in the QuickWave 3D [19] electromagnetic environment in order to verify the results and propose a close-form formula to calculate the height of posts that need to be added to hemispherical lenses. Fig. 2(b) shows the power density distribution within a synthesized lens, as well as within a matching reference elliptical lens of a diameter of 4 mm illuminated with a plane wave of a frequency of 340 GHz. Two red crosses mark the expected location of the foci within the elliptical lens based on [18]. As shown, the location of the lower focus within the synthesized lens has moved slightly towards the center of the lens (and away from the flat bottom) but the power density observed there is comparable to that within the full elliptical lens.

Using the numerical model a number of synthesized lenses of different diameters D has been analyzed for power density distribution and the location of the lower focus. The results have been shown in Fig. 4(a) in the logarithmic scale which is better suited to comparing power densities that are varying rapidly. Additionally, the model has been also used to investigate the consequences of employing a post that is too short or two long as compared to the optimal one. An exemplary lens of dimensions of 4 mm has been used in the numerical experiment. The results are presented in Fig. 4(b). It seems that the system is quite sensitive to the location of the flat bottom as the power density observed in the lower focus of the analyzed lens can change even by a factor of 2–3 when the post is extended (or shortened) even by 0.1 mm. What is important, however, is that the power density measured at the flat bottom of the lens the differences are much smaller. Practice-wise, this location is more important than the focus as this is where the antenna of the detector can be installed on the lens, while there is no access to the focus.

Based on the numerical calculations for a number of various lenses it is possible to propose a simplified formula to calculate the height L of the post added to a hemispherical lens so that the flat bottom of the resulting lens is found at the same height as the analytical focus of the reference elliptical lens. It turned out that height L is linearly dependent on the lens diameter and the relationship is $L = 0.19646 \times D$. In our experiment we needed a lens of a diameter of 10 mm for the height L. Thus, the height L should be 1.96 mm and in order to synthesize a proper lens we have chosen a hyper-spherical lens of a diameter of 10 mm of overall height 7 mm. The chip with the log-periodic antenna is 70-micron-thick which brings the focal plane at a distance that is only approx. 30 μm shifted away from the optimal position.

5. Results and discussion

The I–V curves obtained with the set-up (using the GSG probes) for each structure are presented in Fig. 3(a) . The photo-detection signal measured during responsivity characterization has been recorded at the V_{GS} voltage corresponding to maximum responsivity (i.e., the knee voltage at ca. −0.3 V). This has been illustrated in

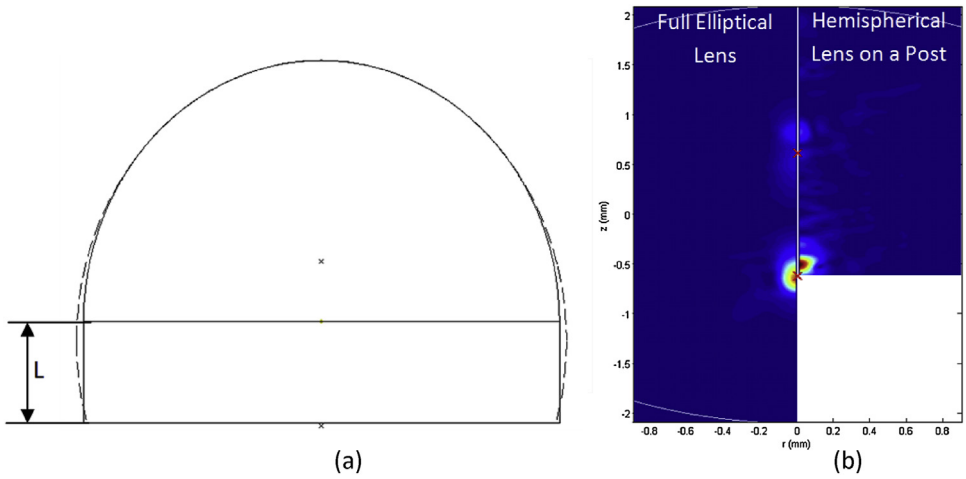

Fig. 3. The shape of synthesized lens built of a hemispherical lens and a post (solid line) compared to the shape (dashed line) of a reference elliptical lens (a) and power density distribution within the synthesized lens and a matching reference elliptical lens of diameter of 4 mm illuminated with 340 GHz (b).

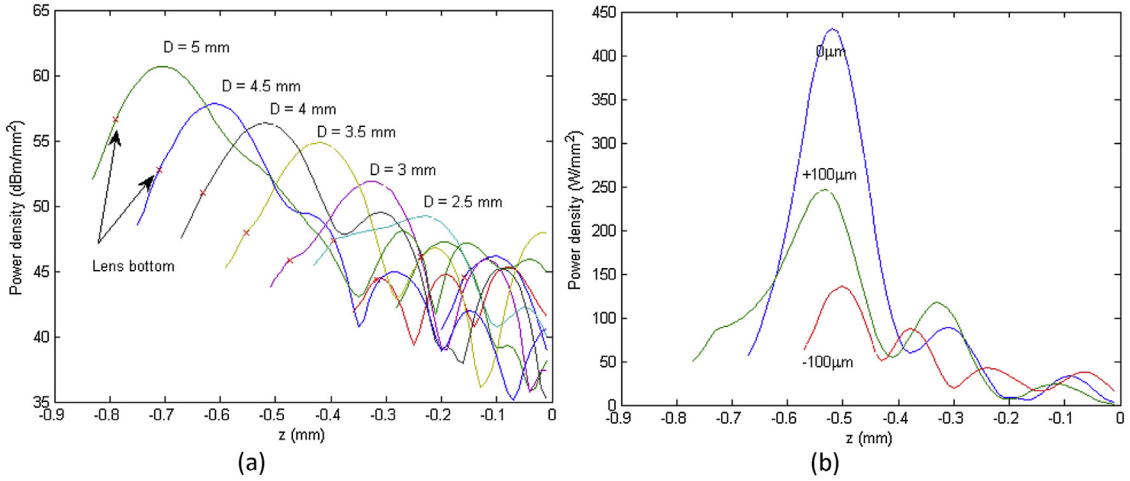

Fig. 4. Power density distribution along the axes of synthesized lenses of various diameters (a) and dependence of power density distributions for a exemplary lens of diameter 4 mm for different heights of the extension post L varying around the location of the analytical focus of a matching elliptical lens (b).

Fig. 3(a) showing responsivity measured at 220 GHz *vs*. the biasing voltage. The $|S_{11}{}^{FET}|$ measured during a separate campaign using a VNA averages to the value of ca. 0.6. While calculating the responsivity R with Eq. (1), the $S_{21}{}^{Att}$ factor has been corrected to account for non-ideal probe-DUT contact, as well as the reflections from the devices have been accounted for with the $|S_{11}{}^{FET}|$ coefficient. The measured responsivity is shown in Fig. 3(b). The obtained level of ca. 300 V/W in the frequency range of WR-3 suggests that HEMT GaAs devices fabricated with commercial processes are comparable to Schottky diodes in terms of the observed responsivity.

Comparing the photo-detection voltage VDS obtained from the HEMT-based device with the photo-response obtained from the VDI's device allows us to determine the responsivity of our detector using Eq. (3). The VDI's quasi-optical products are characterized using waveguide detectors as in Ref. 4, and their responsivity in (V/W) is provided in the specification data [20]. The responsivity of our HEMT-based detector measured in the WR-3 using the comparative approach is ca. 30 V/W. The measured photo-detection signals recorded in the same measurement set-up for two detectors have been presented in Fig. 3(a), while the calculated responsivity is shown in Fig. 3(b).

Given the fact that the diameters of the lenses employed in the analyzed detectors are very similar, neither is covered with anti-reflection coating and are both made of HR-Si, which is a low-loss material whose properties are not known to change considerably from batch to batch, it can be safely assumed that comparable power density is observed in the lower foci of both lenses. The observed 10-fold reduction of the responsivity of the complete detector from the value measured for the bare HEMT transistor with the on-wafer approach require a systematic study to be published in a separate article. It can be assumed that effects reducing the overall responsivity from the expected level of 300 V/W are occurring at the interface between the log-periodic antenna and the bottom of the lens, as well as at the interface between the antenna and the HEMT device.

For example, the input impedance of similar log-periodic antennas fabricated on materials with the relative permittivity $\varepsilon_r = 12$ (as is the case of GaAs) is known to be ca. 50 Ω [15]. The characteristic impedance of GSG probes used in the on-wafer measurement campaign described in Section 2. is also 50 Ω, which means that the value of the coefficient $|S_{11}{}^{FET}|$ measured previously roughly defines the impedance mismatch between the antenna and the HEMT transistor. The mismatch would reduce the amount of power that is delivered to its active part of the transistor by half limiting also the overall responsivity by the same factor. Any similar effect would further reduce the overall responsivity bringing it from the best-case level measured using the on-wafer approach down (Figs. 5 and 6).

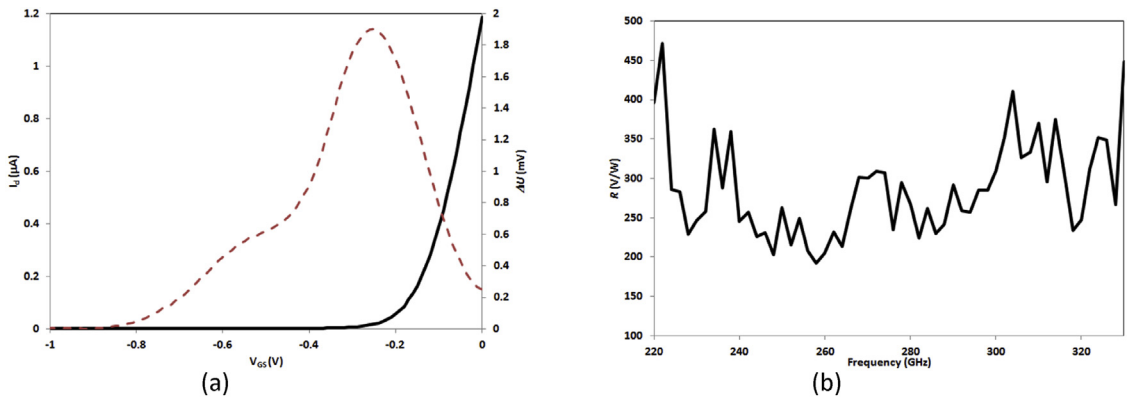

Fig. 5. The I–V characteristics (measured at V_{DS} = 50 mV) of the DUT compared to the amplitude of the photo-detection signal measured at the frequency of 220 GHz (a) and the responsivity of the DUT measured in the WR-3 frequency band at the biasing voltage V_{GS} set at ca. -0.3 V (b).

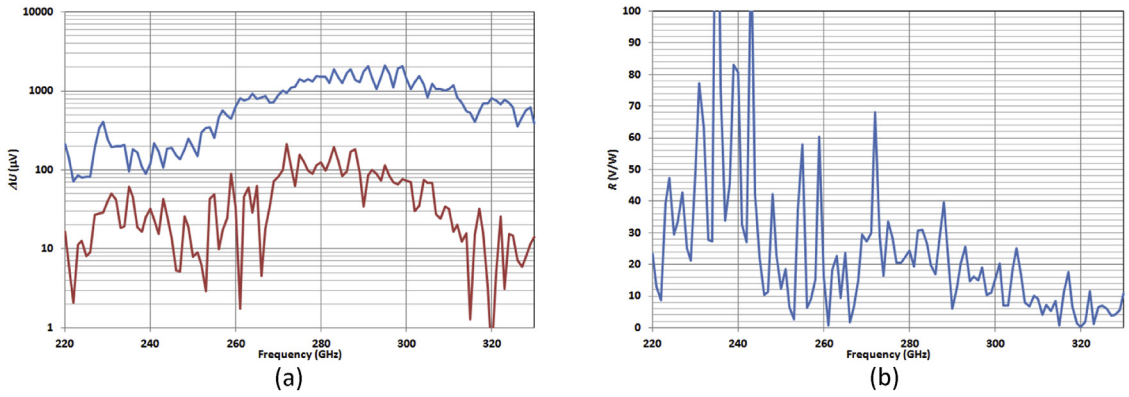

Fig. 6. The photo-detection signal of a detector with DUT or the reference and recorded vs. frequency (a) and estimated responsivity of the DUT based on specifications of the reference detector (b).

6. Conclusions

In this paper a novel on-wafer approach to responsivity measurements of FET-based detectors has been proposed and demonstrated. With the rigorous method we have measured devices fabricated with a 100 nm pHEMT commercial process. As a result we could obtain a best-case estimate of the responsivity that could be achieved by sub-THz radiation detectors built using similar devices. Our results are rather far from theoretical limits predicted by the DS theory and have been validated by an alternative approach to responsivity measurement of sub-THz quasi-optical detectors. The second method presented here is based on a straightforward comparison of the performance of two quasi-optical broad-band detectors. The first of those detectors has been built using a transistor fabricated with the same pHEMT process as the devices employed in the on-wafer measurement campaign. The second one is a commercial detector based on state-of-the-art Schottky diode and its responsivity is known and specified by the manufacturer. Similar detectors can be found in many sub-THz and far-infrared research laboratories around the world. Provided that the power density of the illuminating wave is the same in both cases, the proposed approach allows extracting the responsivity of the unknown detector without need for any arbitrary coefficients like A_{eff}.

Acknowledgements

This work was partially supported by the National Center for Research and Development in Poland under the LIDER/020/319/L-5/13/NCBR/2014 contract and by the Foundation for Polish Science as the grant no TEAM-TECH/2016-1/3.

References

[1] M. Dyakonov, M. Shur, Detection, mixing, and frequency multiplication of terahertz radiation by two-dimensional electronic fluid, IEEE Trans. Electron Devices 43 (3) (1996) 380–387.
[2] S. Boppel, et al., CMOS integrated antenna-coupled field-effect transistors for the detection of radiation from 0.2 to 4.3 THz, IEEE Trans. Microw. Theory Technol. 60 (12) (2012) 3834–3843.
[3] P.H. Siegel, Terahertz technology, IEEE Trans. Microw. Theory Technol. 50 (3) (2002) 910–928.
[4] J.L. Hesler, L. Liu, H. Xu, Y. Duan, R.M. Weikle, The development of quasi-optical THz detectors, in: 33rd International Conference on Infrared and Millimeter Waves and the 16th International Conference on Terahertz Electronics, 1-3, IRMMW-THz, 2008.
[5] J. Marczewski, W. Knap, D. Tomaszewski, M. Zaborowski, P. Zagrajek, Silicon junctionless field effect transistors as room temperature terahertz detectors, J. Appl. Phys. 118 (2015) 104502.
[6] W. Knap, et al., Nonresonant detection of terahertz radiation in field effect transistors, J. Appl. Phys. 91 (2002) 9346.
[7] M. Sakowicz, J. Łusakowski, K. Karpierz, M. Grynberg, W. Knap, W. Gwarek, Polarization sensitive detection of 100 GHz radiation by high mobility field-effect transistors, J. Appl. Phys. 104 (2008) 024519.
[8] U.R. Pfeiffer, E. Öjefors, A 600-GHz CMOS focal-plane array for terahertz imaging applications, in: in ESSCIRC 2008 - Proceedings of the 34th European Solid-State Circuits Conference, 2008.
[9] R. Al Hadi, et al., A broadband 0.6 to 1 THz CMOS imaging detector with an integrated lens, IEEE MTTS Int. Microw. Symp. (2011).
[10] F. Schuster, et al., A broadband THz imager in a low-cost CMOS technology, in: Digest of Technical Papers-IEEE International Solid-State Circuits Conference, 2011.
[11] R. Jain, H. Rucker, U.R. Pfeiffer, Zero gate-bias terahertz detection with an asymmetric NMOS transistor, in: International Conference on Infrared, Millimeter, and Terahertz Waves, IRMMW-THz, 2016.

[12] E. Öjefors, N. Baktash, Y. Zhao, R. Al Hadi, H. Sherry, U.R. Pfeiffer, Terahertz imaging detectors in a 65-nm CMOS SOI technology, in: ESSCIRC 2010 - 36th European Solid State Circuits Conference, 2010, 486–489.
[13] P. Kopyt, et al., On-wafer measurements of responsivity of FET-based subTHz detectors, in: IEEE MTT-S International Microwave Symposium Digest, 2018, 946–948, 2018–June.
[14] P. Kopyt, B. Salski, J. Cuper, P. Zagrajek, J. Bar, D. Obrebski, Broadband quasi-optical sub-THz detector based on GaAs HEMT, in: MIKON 2018 - 22nd International Microwave and Radar Conference, 2018, 159–160.
[15] C.A. Balanis, Antenna Theory: Analysis and Design, 3rd edition, Wiley-Interscience, USA, 2005, 3rd Edition.
[16] Nominal Horn Specifications, Virginia Diodes Inc., 1998.
[17] E. Hecht, Optics, Addison Wesley, 1998.
[18] D.F. Filipovic, S.S. Gearhart, G.M. Rebeiz, Double-slot antennas on extended hemispherical and elliptical silicon dielectric lenses, IEEE Trans. Microw. Theory Technol. 41 (10) (1993) 1738–1749.
[19] QuickWave 3D, 2018.
[20] User Guide for the 100-1000GHz Quasi-Optical Detector with Internal ESD Protection, 2011.